

An Analytical Neighborhood Enrichment Score for Spatial Omics

Axel Andersson^{1,*} and Hanna Nyström¹

¹Department of Diagnostics and Intervention, Surgery

Umeå University, Umeå, Sweden

*Corresponding author: axel.andersson@umu.se

Abstract

The neighborhood enrichment test is used to quantify spatial enrichment and depletion between spatial points with categorical labels, which is a common data type in spatial omics. Traditionally, this test relies on a permutation-based Monte Carlo approach, which tends to be computationally expensive for large datasets. In this study, we present a modified version of the test that can be computed analytically. This analytical version showed a minimum Pearson correlation of 0.95 with the conventional Monte Carlo-based method across eight spatial omics datasets, but with substantial speed-ups. Additional experiments on a large Xenium dataset demonstrated the method’s ability to efficiently analyze large-scale data, making it a valuable tool for analyzing spatial omics data.

1 Introduction

Spatial omics, the study of the spatial organization of biomolecules, is a rapidly growing field [1]. Many spatial omics techniques produce image data that, after analysis, yield spatial points with categorical labels. For example, these points may represent locations of different cell types or mRNA molecules.

The neighborhood enrichment test [2] is a widely used permutation-based method to quantify spatial enrichment or depletion between points with different labels. It is implemented in several statistical toolboxes for spatial omics [2, 3, 4, 5] and has been applied in numerous studies [6, 7]. The test measures how often spatial points with label A are neighbors to those with label B, then compares this observed count to a null distribution generated by repeatedly shuffling the labels across the data set. The output is a z-score-like value that indicates whether the two labels are spatially enriched or de-

pleted. However, the repeated shuffles required to estimate this distribution can be computationally intensive, particularly for large datasets with many labels. We therefore propose a modified version of the enrichment score that can be computed analytically. This approach significantly improves computational speed and scalability. The code is publicly available at <https://github.com/wahlby-lab/analytical-enrichment-test>.

2 Materials and methods

The neighborhood enrichment score

The enrichment score, as implemented in the popular spatial omics toolbox Squidpy [2], is given by:

$$z_{AB} = \frac{x_{AB} - \mu_{AB}}{\sigma_{AB}} \quad (1)$$

where x_{AB} is the count of points with label A that are neighbors points with label B. A neighbor can be defined in different ways, for example, if two points are within a set distance or if a point is within the k -nearest neighbors of a reference point. The variables μ_{AB} and σ_{AB} in Eq. 1 correspond to the expectation and standard deviation in the number of neighbors between A-labeled points and B-labeled points after shuffling the labels of the points. The number of shuffles, N_{MC} , used to estimate μ_{AB} and σ_{AB} is given as a user-defined parameter and should be large to avoid a high variance in the estimated z scores. Default in Squidpy is $N_{MC} = 10^3$ [2].

Analytical neighborhood enrichment score

Instead of shuffling the labels and estimating the mean and standard deviation of neighbor counts through Monte Carlo sampling, we propose an analytical alternative that can be computed directly. Consider two labels: a reference label A, and a neighbor label B, and define:

- $\mathbf{b} \in \{0, 1\}^N$: a binary vector indicating which of the N points have label B,
- $\mathbf{W} \in \{0, 1\}^{N \times N}$: a sparse adjacency matrix encoding the neighborhood graph,
- $\mathbf{1} \in \mathbb{R}^N$: a vector of ones (i.e., $\mathbf{1}_i = 1$ for all i).

The vector containing the number of B-labeled neighbors for each point is:

$$\mathbf{y} = \mathbf{W}\mathbf{b}.$$

The expected number of B-labeled neighbors for a randomly selected point is:

$$\mathbb{E}[\mathbf{y}] = \frac{1}{N} \mathbf{1}^\top \mathbf{y},$$

and the variance is:

$$\mathbb{V}[\mathbf{y}] = \mathbb{E}[\mathbf{y}^{\circ 2}] - \mathbb{E}[\mathbf{y}]^2,$$

where $(\cdot)^{\circ 2}$ refers to the Hadamard square. Let n_A be the number of points with the label A. If we sample n_A points independently with replacement, the expected total number of B-labeled neighbors is:

$$\mu_{AB} = n_A \cdot \mathbb{E}[\mathbf{y}],$$

with variance:

$$\sigma_{AB}^2 = n_A \cdot \mathbb{V}[\mathbf{y}].$$

The proposed analytical enrichment z-score is then given by:

$$z_{AB} = \frac{o_{AB} - \mu_{AB}}{\sigma_{AB}}, \quad (2)$$

where o_{AB} is the total number of neighbors labeled B of points labeled A, computed as:

$$o_{AB} = \mathbf{a}^\top \mathbf{y}.$$

with $\mathbf{a} \in \{0, 1\}^N$ as the indicator vector for label A points. Equation 2 can be rewritten as:

$$z_{AB} = \sqrt{n_A} \cdot \frac{\bar{o}_{AB} - \mathbb{E}[\mathbf{y}]}{\sqrt{\mathbb{V}[\mathbf{y}]}}$$

where $\bar{o}_{AB} = \frac{o_{AB}}{n_A}$.

Matrix formulation of the enrichment score

The previous pairwise formulation can be extended to a matrix-based form that simultaneously computes enrichment scores for all label pairs using basic linear algebra. Define:

- $\mathbf{L} \in \{0, 1\}^{N \times K}$: a one-hot label matrix, where $L_{ik} = 1$ if the point i has the label k and K is the number of unique labels.

Table 1: Dataset characteristics including the number of unique labels and total number of points.

Dataset	# of labels	# of points	Ref.
MIBI-TOF	8	1.2k	[8]
4i	15	2.8k	[9]
Visium	12	2.8k	[10]
IMC	11	4.7k	[11]
MERFISH I	16	6.5k	[12]
SeqFISH	22	19.4k	[13]
osmFISH	36	1.98M	[14]
MERFISH II	135	3.73M	[12]

- $\mathbf{N} = \text{diag}(\mathbf{L}^\top \mathbf{1}) \in \mathbb{N}^{K \times K}$: a diagonal matrix where N_{kk} is the number of points with the label k .

The matrix of neighbor label counts is given by:

$$\mathbf{Y} = \mathbf{W}\mathbf{L} \in \mathbb{R}^{N \times K}, \quad (3)$$

where each column $\mathbf{Y}_{:,k}$ contains the number of neighbors with label k for each point. The observed number of neighbors labeled k for each point labeled j is given by the matrix:

$$\mathbf{O} = \mathbf{L}^\top \mathbf{Y} = \mathbf{L}^\top \mathbf{W}\mathbf{L} \in \mathbb{R}^{K \times K}$$

and the corresponding per-point average is:

$$\bar{\mathbf{O}} = \mathbf{N}^{-1} \mathbf{O}.$$

The matrix of enrichment z-scores between all pairs of labels is:

$$\mathbf{Z} = \mathbf{N}^{1/2} \left(\frac{\bar{\mathbf{O}} - \mathbb{E}[\mathbf{Y}]}{\sqrt{\mathbb{V}[\mathbf{Y}]}} \right) \in \mathbb{R}^{K \times K},$$

where all square roots, divisions, and differences are applied element-wise. Here, $\mathbb{E}[\mathbf{Y}] \in \mathbb{R}^{1 \times K}$ and $\mathbb{V}[\mathbf{Y}] \in \mathbb{R}^{1 \times K}$ are the expected values and variances of \mathbf{Y} across all points, calculated column-wise.

3 Experiments and results

To evaluate the performance of the analytical neighborhood enrichment test, we compared it to the original Monte Carlo-based approach implemented in Squidpy [2]. Our objectives were twofold: (i) to assess whether the two methods yield similar results by comparing their z-scores, and (ii) to quantify the computational speed-up achieved by the analytical method.

We analyzed eight spatial omics datasets (Table 1) using k -nearest neighbor graphs with $k = 6, 12$, and 18 to define the neighborhoods. For each dataset, we ran the Monte

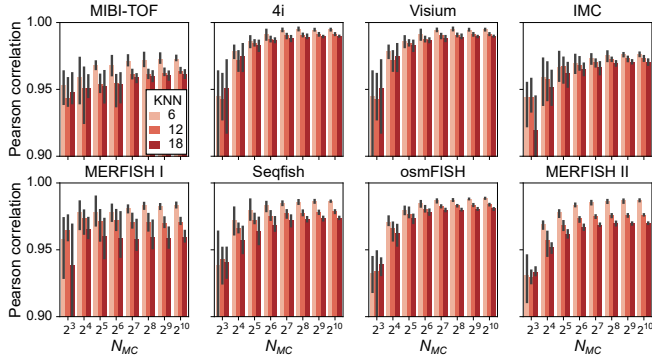
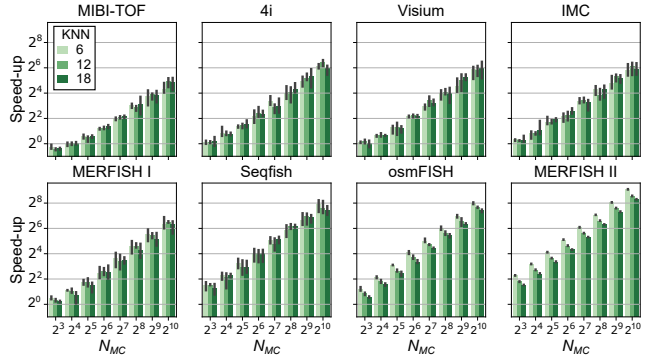
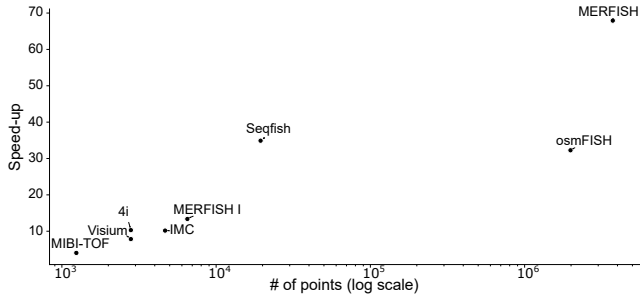
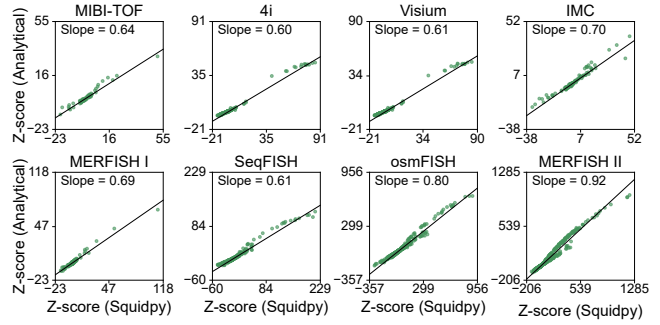
A Person correlation between Analytical and Monte Carlo**B** Speed-up of Analytical vs Monte Carlo**C** Speed-up vs dataset size ($N_{MC} = 128, k = 6$)**D** Z-score comparison ($N_{MC} = 128, k = 6$)

Figure 1: The analytical enrichment score shows strong agreement with traditional Monte Carlo-based method across multiple datasets, while providing substantial speed-up. **A** Pearson correlation between the proposed Analytical enrichment score and the Monte Carlo-based implementation in Squidpy [2] with different number of label-permutations (N_{MC}). **B** Speed-up of the analytical method compared to the Monte Carlo-based approach. Experiments were conducted using neighborhood graphs constructed with $k = 6, k = 12$, or $k = 18$ nearest neighbors. **C** Speed-up of the analytical method compared to the Monte Carlo-based method for different dataset sizes (number of points). Speed-up increased with dataset size. **D** Comparison of z-scores computed by the analytical and Monte Carlo-based methods. Each point represents the enrichment z-score for a pair of labels in a given dataset. Overall, the z-scores produced by the analytical methods are lower than those of the Monte Carlo-based method.

Carlo-based method with $N_{MC} = 2^i$ label permutations, where $i = 3, \dots, 10$ (i.e., N_{MC} ranging from 8 to 1024). Using both methods, we computed z-scores for all label pairs and assessed their agreement via Pearson correlation. To account for the stochastic nature of the Monte Carlo approach, we averaged results over five independent runs. Figure 1A shows the mean correlation, with error bars indicating the range (max–min) across repetitions. In all datasets, the correlation seemed to plateau after $N_{MC} = 128$, and exceeded 0.95 in all cases, indicating a strong agreement between the methods.

Next, to assess computational efficiency, we measured the speed-up factor:

$$\text{Speed-up} = \frac{T_{\text{Monte Carlo}}}{T_{\text{Analytical}}},$$

where $T_{\text{Monte Carlo}}$ and $T_{\text{Analytical}}$ denote the runtimes of the respective methods. As before, speed-ups were averaged

over five repetitions, with ranges shown as error bars. Figure 1B illustrates how the speed-up increases with N_{MC} , as expected, and tends to be higher for larger datasets (e.g., MERFISH II) and smaller ones, where overhead dominates.

To further explore the relationship between speed-up and dataset size, we fixed $N_{MC} = 128$, after which the Monte Carlo results had stabilized (as noted in Figure 1A), and computed the speed-up for $k = 6$. Figure 1C shows the resulting speed-up as a function of dataset size, confirming that the speed-up is greater for large datasets.

Lastly, we noted that the z-scores given by the analytical method were slightly lower than those produced by the Monte Carlo-based method, see Figure 1D.

Analytical neighborhood enrichment score on Xenium data

Finally, we tested the scalability of the analytical neighborhood enrichment score on a large-scale Xenium dataset. We used the Fresh Frozen Mouse Brain for Xenium Explorer Demo, publicly available at <https://www.10xgenomics.com/datasets>. This dataset contains 248 mRNA labels and over 40 million spatial points. Using a $k = 6$ nearest neighbor graph and running the computation on a machine with an AMD Ryzen 7 7840HS processor with Radeon 780M Graphics (3.80 GHz) and 16 GB of RAM, the analytical enrichment computation took approximately 90 seconds (excluding graph construction time).

4 Discussion

In this short work, we proposed an analytical version of the neighborhood enrichment score, providing a fast alternative to the Monte Carlo-based method. Our approach yields enrichment scores that are highly correlated with those from the original Monte Carlo sampling method while offering substantial computational speed-up.

Both the Monte Carlo and analytical methods have time complexity proportional to the number of edges in the neighborhood graph. The Monte Carlo method traverses all E edges and checks the labels of connected points. This process is repeated for each of the N_{MC} label permutations, giving a time complexity of $\mathcal{O}(EN_{MC})$. The analytical method is dominated by the sparse matrix product $\mathbf{W}\mathbf{L}$, which also has complexity $\mathcal{O}(E)$ since each non-zero in \mathbf{W} touches a single non-zero in \mathbf{L} exactly once.

If N_{MC} is fixed, this suggests a constant speed-up of the analytical method. However, as shown in Figure 1C, the observed speed-up increases with dataset size. This is likely due to implementation differences: the Monte Carlo method performs sequential edge traversals in Python (optimized with Numba’s just-in-time compiler for performance), while the analytical method uses highly optimized sparse matrix operations (SciPy). For small datasets, the overhead of constructing sparse matrices can offset these gains.

A 70× speed-up was observed for one of the larger datasets (MERFISH II). Note that we set $N_{MC} = 128$ permutations for the Monte Carlo-based method, while the default in [2] is $N_{MC} = 1000$. The Monte Carlo-based method is relatively efficient because the same set of permutations can be used to estimate the null distribution for all label pairs. By contrast, methods like Ref. [4] uses a different shuffling strategy: the reference label is fixed, and only the neighbor label is permuted. This requires N_{MC} permutations for each label pair, increasing computation time.

Although not explored here, such alternative null models could be incorporated into the analytical method by modifying the expectation $\mathbb{E}[\mathbf{y}]$ to a weighted form.

While the analytical enrichment scores are highly correlated with those from the Monte Carlo method in [2], they tend to be slightly lower (Figure 1D). This difference stems from how label randomization is handled: the Monte Carlo method permutes labels without replacement, preserving label counts, whereas the analytical method samples labels independently based on their observed frequencies (effectively sampling with replacement). As a result, the analytical approach does not constrain label counts, likely leading to higher variance in the null distribution (i.e., larger σ_{AB}), which in turn lowers the resulting z-scores.

The method depends on a single parameter that defines the neighborhood scale, such as k in a k -nearest neighbor graph or a radius in a distance-based graph. This, in combination with the computational efficiency, makes the method easy to use for exploring and quantifying spatial colocalization in the data. However, the spatial distributions of the labels in the omics data are rarely completely random. Different biological structures lead to spatial autocorrelation. Thus, comparing the observed counts of neighboring labels against randomly distributed labels tends to result in significant z-scores. As such, scores are best interpreted as relative indicators of spatial association rather than exact measures of statistical significance.

References

- [1] Dario Bressan, Giorgia Battistoni, and Gregory J Hannon. The dawn of spatial omics. *Science*, 381(6657):eabq4964, 2023.
- [2] Giovanni Palla, Hannah Spitzer, Michal Klein, David Fischer, Anna Christina Schaar, Louis Benedikt Kuemmerle, Sergei Rybakov, Ignacio L Ibarra, Olle Holmberg, Isaac Virshup, et al. Squidpy: a scalable framework for spatial omics analysis. *Nature methods*, 19(2):171–178, 2022.
- [3] Denis Schapiro, Hartland W Jackson, Swetha Raghuraman, Jana R Fischer, Vito RT Zanotelli, Daniel Schulz, Charlotte Giesen, Raúl Catena, Zsuzsanna Varga, and Bernd Bodenmiller. histocat: analysis of cell phenotypes and interactions in multiplex image cytometry data. *Nature methods*, 14(9):873–876, 2017.
- [4] Andrea Behanova, Christophe Avenel, Axel Andersson, Eduard Chelebian, Anna Klemm, Lina Wik, Arne Östman, and Carolina Wählby. Visualization and quality control tools for large-scale multiplex tis-

- sue analysis in tissuumaps3. *Biological Imaging*, 3:e6, 2023.
- [5] Rafael dos Santos Peixoto, Brendan F Miller, Maigan A Brusko, Gohta Aihara, Lyla Atta, Manjari Anant, Mark A Atkinson, Todd M Brusko, Clive H Wasserfall, and Jean Fan. Characterizing cell-type spatial relationships across length scales in spatially resolved omics data. *Nature Communications*, 16(1):350, 2025.
- [6] Srinand Sundaram, Eun Na Kim, Georgina M Jones, Shamilene Sivagnanam, Monika Tripathi, Ahmad Miremadi, Massimiliano Di Pietro, Lisa M Coussens, Rebecca C Fitzgerald, Young Hwan Chang, et al. Deciphering the immune complexity in esophageal adenocarcinoma and pre-cancerous lesions with sequential multiplex immunohistochemistry and sparse subspace clustering approach. *Frontiers in immunology*, 13:874255, 2022.
- [7] Christoffer Mattsson Langseth, Daniel Gyllborg, Jeremy A Miller, Jennie L Close, Brian Long, Ed S Lein, Markus M Hilscher, and Mats Nilsson. Comprehensive in situ mapping of human cortical transcriptomic cell types. *Communications Biology*, 4(1):998, 2021.
- [8] Felix J Hartmann, Dunja Mrdjen, Erin McCaffrey, David R Glass, Noah F Greenwald, Anusha Bhargava, Zumana Khair, Alex Baranski, Reema Baskar, Michael Angelo, et al. Multiplexed single-cell metabolic profiles organize the spectrum of cytotoxic human t cells. *BioRxiv*, pages 2020–01, 2020.
- [9] Gabriele Gut, Markus D Herrmann, and Lucas Pelkmans. Multiplexed protein maps link sub-cellular organization to cellular states. *Science*, 361(6401):eaar7042, 2018.
- [10] Squidpy datasets. <https://squidpy.readthedocs.io/en/stable/api.html#module-squidpy.datasets>. [Accessed 15-01-2024].
- [11] Hartland W Jackson, Jana R Fischer, Vito RT Zantotelli, H Raza Ali, Robert Mechera, Savas D Soysal, Holger Moch, Simone Muenst, Zsuzsanna Varga, Walter P Weber, et al. The single-cell pathology landscape of breast cancer. *Nature*, 578(7796):615–620, 2020.
- [12] Jeffrey R Moffitt, Dhananjay Bambah-Mukku, Stephen W Eichhorn, Eric Vaughn, Karthik Shekhar, Julio D Perez, Nimrod D Rubinstein, Junjie Hao, Aviv Regev, Catherine Dulac, et al. Molecular, spatial, and functional single-cell profiling of the hypothalamic preoptic region. *Science*, 362(6416):eaau5324, 2018.
- [13] Tim Lohoff, Shila Ghazanfar, Alsu Missarova, Noushin Koulana, Nico Pierson, Jonathan A Griffiths, Evan S Bardot, C-HL Eng, Richard CV Tyser, Richard Argelaguet, et al. Highly multiplexed spatially resolved gene expression profiling of mouse organogenesis. *BioRxiv*, pages 2020–11, 2020.
- [14] Simone Codeluppi, Lars E Borm, Amit Zeisel, Gioele La Manno, Josina A van Lunteren, Camilla I Svensson, and Sten Linnarsson. Spatial organization of the somatosensory cortex revealed by osmfish. *Nature methods*, 15(11):932–935, 2018.